Surface Emissivity Derived from Multispectral Satellite Data

P. Minnis and D. F. Young
Atmospheric Sciences Division
NASA-Langley Research Center
Hampton, Virginia

W. L. Smith, Jr.
Analytical Services and Materials, Inc.
Hampton, Virginia

Introduction

Surface emissivity is critical for remote sensing of surface skin temperature and infrared cloud properties when the observed radiance is influenced by the surface radiation. It is also necessary to correctly compute the longwave flux from a surface at a given skin temperature. Surface emissivity is difficult to determine because skin temperature is an ill-defined parameter. The surface-emitted radiation may arise from a range of surface depths depending on many factors including soil moisture, vegetation, surface porosity, and heat capacity. Emissivity can be measured in the laboratory for pure surfaces. Transfer of laboratory measurements to actual earth surfaces, however, is fraught with uncertainties because of their complex nature. This paper describes a new empirical approach for estimating surface skin temperature from a combination of brightness temperatures measured at different infrared wavelengths with satellite imagers. The method uses data from the new Geostationary Operational Environmental Satellite (GOES) imager to determine multispectral emissivities from the skin temperatures derived over the Atmospheric Radiation Measurement (ARM) Southern Great Plains (SGP) domain.

Data

GOES imager solar-infrared (SI, 3.9 μm), infrared (IR, 10.8 μm), and split-window (WS, 11.9 μm) data taken at a nominal 4-km resolution were averaged on a regular 0.5° grid between 32°N and 42°N and between 90°W and 104°W on a half-hourly basis for all grid boxes that were classified as completely clear. The data included April 1996, July and September 1997, and January 1998 to represent the four seasons. Clear regions were determined using the approach of Minnis et al. (1995). The grid-box averaging is performed using pixel radiances. The mean radiance is converted to an equivalent blackbody temperature T_I, where the subscript corresponds to a channel number: 2 for SI, 4 for IR, and 5 for WS.

Derivation of the skin temperature requires correction for the attenuation by atmospheric gases. Water vapor is the primary absorber at these wavelengths. Atmospheric profiles of temperature and humidity were developed from the 60-km resolution ARM-Rapid Update Cycle analyses by interpolation.

Methodology

The radiance exiting the surface for a given channel is

$$B_i(T_{si}) = \varepsilon_i B_i(T_{skin}), \quad (1)$$

where B is the Planck function, ε is the surface emissivity, T_{si} is the apparent surface temperature, and T_{skin} is the skin temperature. The observed radiance is due to a combination of radiances from the surface and atmosphere. In a simple form,

$$B_i(T_i) = \varepsilon_{ai} B_i(T_{ai}) + (1 - \varepsilon_{ai}) B_i(T_{si}), \quad (2)$$

where ε_a and T_a are the effective emissivity and effective temperature of the atmosphere, respectively. Thus, T_{si} can be derived by solving Eq. (2) given the observed radiance, the temperature and humidity profiles, and a means for converting the atmospheric gas concentrations to spectral optical depth. The latter was accomplished using the correlated-k method of Kratz (1995) for the GOES imager channels. The actual solution to Eq. (2) is found by computing the emission and absorption for each of seven atmospheric layers using the correlated-k optical depth of the layer. Sequential removal of the contribution and absorption of each layer from the observed radiance down to the surface yields T_{si}.

A more specific formulation of Eq. (1) for the IR channel yields

$$T_{skin} = B_4^{-1}\{B_4(T_{s4}) / \varepsilon_4)\} \quad (3)$$

for any time of day. Similarly,

$$\varepsilon_2 = B_2 (T_{s2}) / B_2(T_{skin}) \quad (4)$$

at night. Using the atmospheric corrections for each channel to obtain the apparent surface temperatures in each channel, it is possible to define the apparent SI emissivity as

$$\varepsilon_2' = B_2(T_{s2}) / B_2(T_{s4}), \quad (5)$$

a value that can be easily computed at night from the observations. During the daytime, solar radiation is reflected from the surface in channel 2. The surface reflectance is

$$\rho_2 = \chi \alpha_2, \quad (6)$$

where $\chi(\mu_0,\mu,\psi)$ is the anisotropic correction factor, μ_0 and μ are the cosines of the solar and viewing zenith angles, ψ is the relative azimuth angle, and α is the surface albedo. Thus, the apparent surface temperature in channel 2 is

$$B_2(T_{s2}) = \varepsilon_2\{B_2(T_{skin})\} + \alpha_2 \chi S_2', \quad (7)$$

where the solar radiance reaching the surface S_2' is the channel-2 solar constant adjusted for the Earth-Sun distance and solar zenith angle and attenuated by atmospheric absorption using the correlated-k optical depths. Neglecting any solar-zenith angle dependence and invoking Kirchhoff's law, the surface albedo is

$$\alpha_2 = (1 - \varepsilon_2). \quad (8)$$

If it is assumed that the apparent emissivity is constant, then by rearranging Eqs. (4), (5), and (8) and substituting into Eq. (7), the apparent channel-2 radiance from the surface can be approximated as

$$B_2(T_{s2}) = \varepsilon_2'\{B_2(T_{s4})\} + (1 - \varepsilon_2) \chi S_2'. \quad (9)$$

By deriving an average value of ε_2' from nighttime clear data, the true surface emissivity can be determined from Eq. (9) using daytime data. The skin temperature can then be computed from Eq. (4) and the emissivity in any channel can be determined using Eq. (1).

A value of ε_2' was computed for each box at every nocturnal time period when the box was totally clear. These values were then averaged to obtain a mean apparent emissivity for each box during a given month. The averaged values were then used to determine a value of ε_2 from Eq. (9) for every time when $\mu_o > 0.2$ and the region was totally clear. Means and standard deviations of ε_2 were then computed for each region. Similarly, mean values for ε_4 and ε_5 were derived from Eqs. (4) and (1) after ε_3 was determined for each set of clear observations. Because of a lack of knowledge of the bidirectional reflectance patterns at 3.9 μm, the visible-channel bidirectional reflectance model described by Minnis and Harrison (1984) was used for χ. A radiance equivalent to a blackbody temperature of 344.8 K was used for the channel-2 solar constant.

Results

Figure 1 shows the mean channel-2 emissivities derived from daytime data. In general, ε_2 ranges from 0.85 to 0.99 decreasing from east to west. The smallest values are found over the high plains of Texas and, overall, during April. The largest values are primarily found in the forested areas of the east during July. The emissivities appear to be well-correlated with vegetation type: forested areas having values around 0.96-0.99, drier grasslands with values around 0.89, and croplands around 0.95. During January, snow over parts of central Colorado and eastern Iowa gives rise to $\varepsilon_2 \sim 0.99$. The seasonal cycle appears to follow the greening of the local vegetation. The large values of ε_2 in southern Arkansas during January occur in areas dominated by evergreen coniferous forests.

The variability of ε_2 within a given month is represented by the standard deviations σ shown in Figure 2. Except for areas with snow, the variability during January is relatively small with $\sigma < 0.03$. It is also fairly small during April except over northern Texas. During July and September, σ varies between 0.02 and 0.05, except at the edge of the Rocky Mountains. The largest values may be related to changes in soil moisture or vegetation due to crop harvesting or plowing.

The emissivities for two channels can also be derived using nighttime data with the emissivity derived from daytime data for the third channel. The nighttime ε_2 values were derived from the nocturnal data using ε_4 based on the daytime data. Assuming no diurnal effects from soil moisture and solar zenith angle dependence, the values of ε_2 should be the same both day and night. In general, the day and night values differ by no more than 0.01 with larger values during the day.

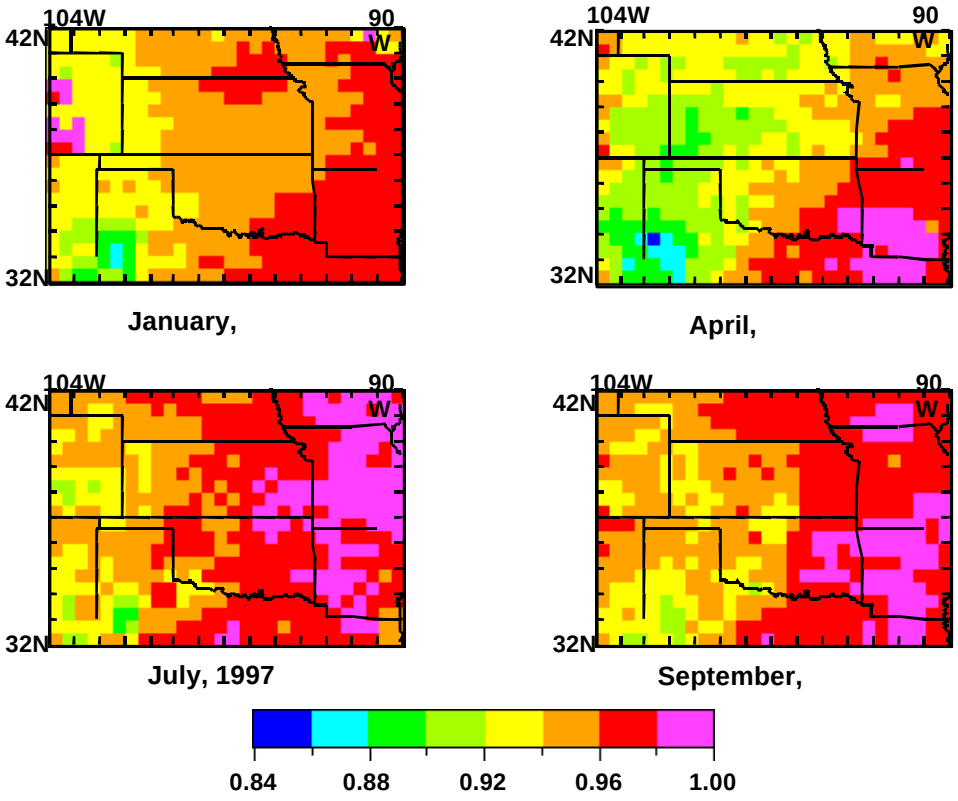

Figure 1. 3.9-μm daytime surface emissivity derived from GOES-8. (For a color version of this figure, please see *http://www.arm.gov/docs/documents/technical/conf_9803/minnis-98.pdf*.)

The nighttime channel-4 emissivities in Figure 3 generally show the same patterns as seen for ε_2, except that ε_4 ranges only from 0.97 to almost 1.0. The daytime values are very similar. The standard deviations for ε_4 are almost the same as those in Figure 2 because the apparent emissivity connects both ε_2 and ε_4. Nocturnal emissivities for channel 5 also follow patterns that are similar to those in Figures 1 and 4, except the range in ε_5 is from 0.95 to 1.0. These emissivities also appear much noisier spatially than the others. Channel 5 is more strongly affected by atmospheric water vapor absorption than the other channels. Thus, any small-scale variability in the moisture field that is not correctly portrayed in the sounding data will have a significant impact on the derived value of ε_5.

The mean domain emissivities in Figure 5 show clearly that the greatest spatial variation occurs simultaneously with the minimum mean value during April. The increased vegetation during the summer and early fall is reflected in the larger emissivities in both channels 2 and 4.

Conclusions

One of the primary uses of the multispectral surface emissivities is the simulation of top-of-atmosphere multispectral radiances or equivalent blackbody temperatures. To determine the accuracy of the simulated temperatures, the monthly mean IR emissivities were used to determine T_{skin} from T_4 for each of the clear hours during the month (same as those used in the original estimate of ε_i). Values of T_2 and T_5 were then computed during the day and night and compared to the observed values. The results summarized in Figures 6 and 7 for channels 2 and 5, respectively, indicate that the derived emissivities can reproduce the observed channel-2 clear-sky temperatures to within 1 K to 2 K during the day depending on the season. The nighttime temperatures are within 0.4 K to 0.9 K. Channel-5 temperature uncertainties are much smaller (within 0.2 K to 0.5 K), but are biased by 0.2 K to 0.5 K on average.

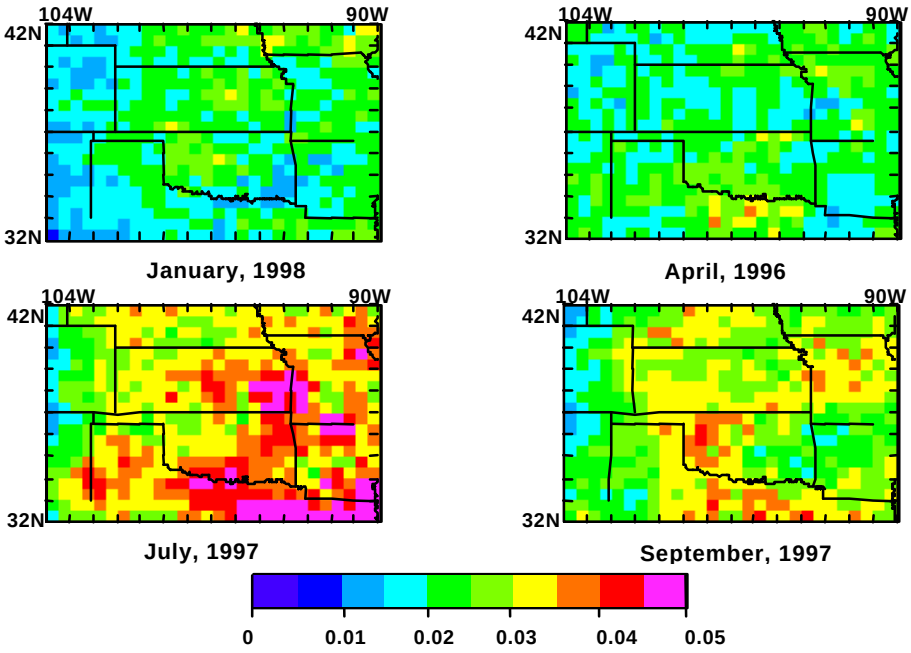

Figure 2. Standard deviation of 3.9-µm daytime surface emissivity from GOES-8. (For a color version of this figure, please see *http://www.arm.gov/docs/documents/technical/conf_9803/minnis-98.pdf*.)

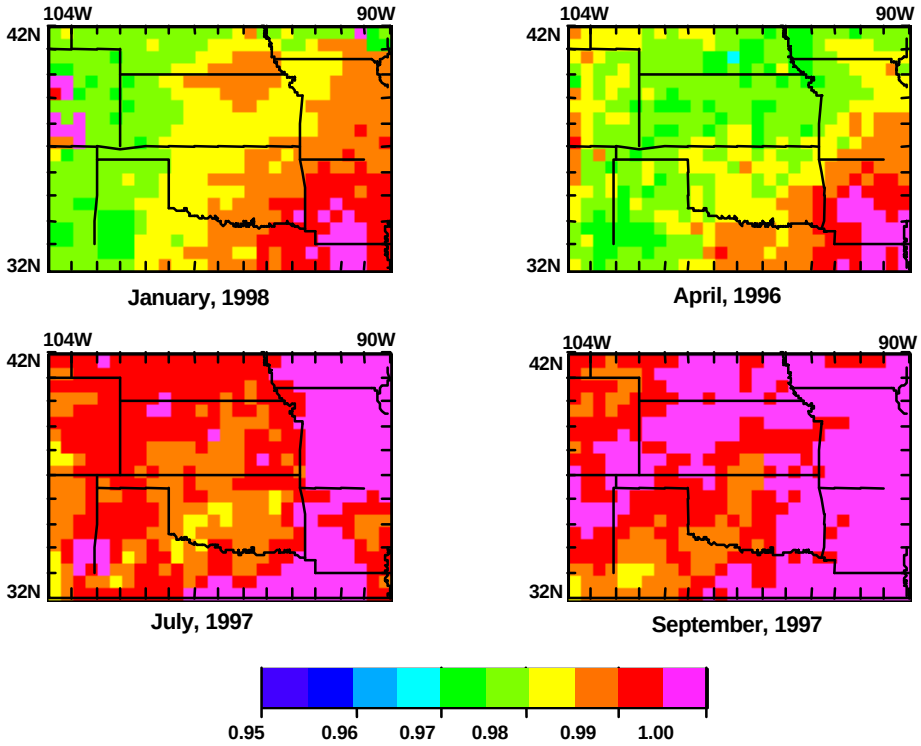

Figure 3. 10.8-µm surface emissivity from nighttime GOES-8 data. (For a color version of this figure, please see *http://www.arm.gov/docs/documents/technical/conf_9803/minnis-98.pdf*.)

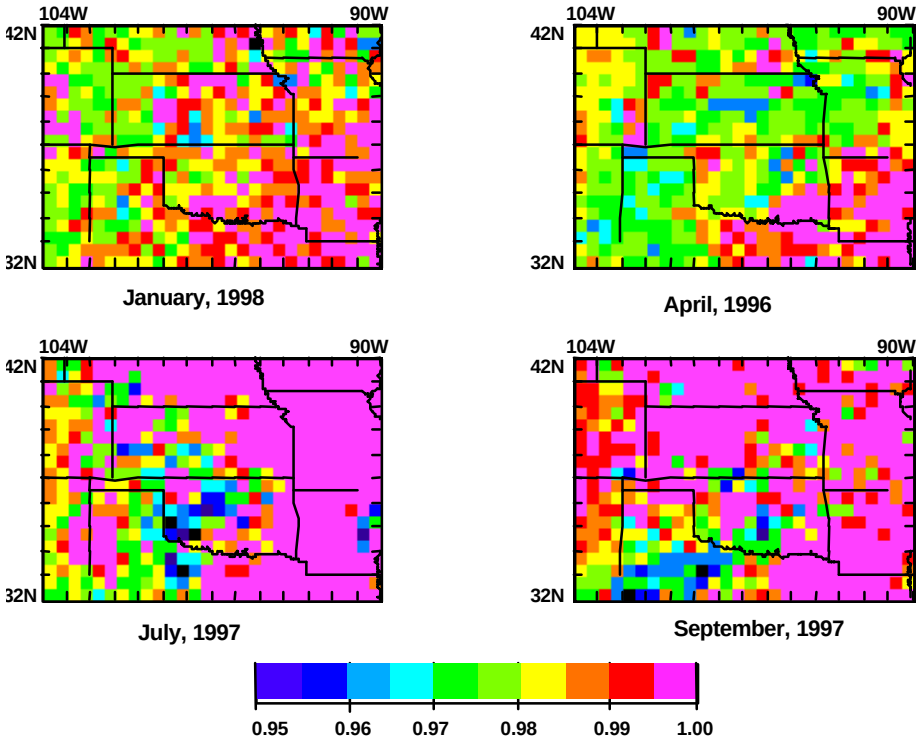

Figure 4. 11.9-µm surface emissivity from nighttime GOES-8 data. (For a color version of this figure, please see *http://www.arm.gov/docs/documents/technical/conf_9803/minnis-98.pdf*.)

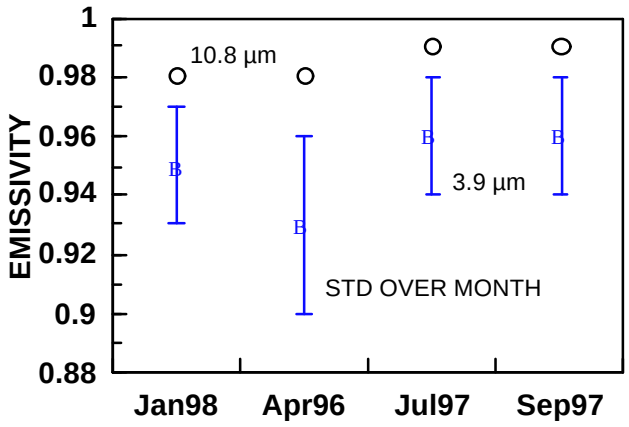

Figure 5. Mean domain surface emissivities. (For a color version of this figure, please see *http://www.arm.gov/docs/documents/technical/conf_9803/minnis-98.pdf*.)

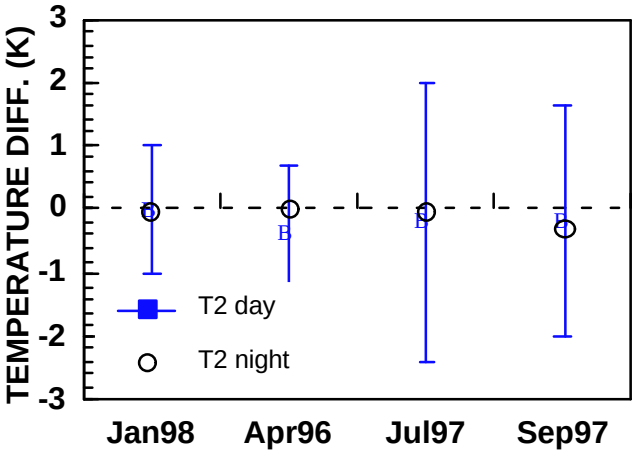

Figure 6. Difference between observed and predicted channel-2 clear-sky temperatures. (For a color version of this figure, please see *http://www.arm.gov/docs/documents/technical/conf_9803/minnis-98.pdf*.)

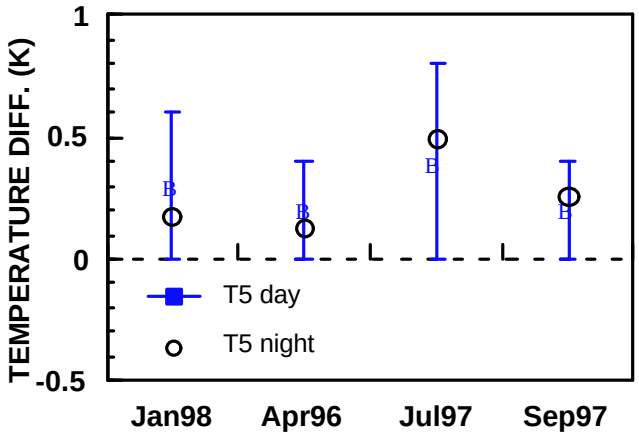

Figure 7. Same as Figure 6 except for channel 5. (For a color version of this figure, please see *http://www.arm.gov/docs/documents/technical/conf_9803/minnis-98.pdf*.)

The biases in the channel-5 temperatures may be due, in part, to the problems of atmospheric humidity noted earlier. Other contributors to the uncertainties in all of the predictions may include the lack of a solar-zenith angle dependence of the albedo, soil moisture and vegetation variations, inadequacy of the assumption of a constant apparent emissivity, and errors in the assumed bidirectional reflectance model. These factors will be explored further to improve the determination of surface emissivity. Data from other months will be used to test the derived emissivities.

Although preliminary, the results strongly support the approach developed here for deriving multispectral surface emissivities.

Acknowledgments

This research was conducted under DOE Interagency Agreement DE-AI05-95ER61992 as part of the ARM/ Unmanned Aerospace Vehicle (UAV) Program.

References

Kratz, D. P., 1995: The correlated k-distribution technique as applied to the AVHRR channels. *J. Quant. Spectrosc. Rad. Transf.*, **53**, 501-507.

Minnis, P., and E. F. Harrison, 1984: Diurnal variability of regional cloud and clear-sky radiative parameters derived from GOES data; Part III: November 1978 radiative parameters. *J. Climate Appl. Meteorol.*, **23**, 1032-1052.

Minnis, P., W. L. Smith, Jr., D. P. Garber, J. K. Ayers, and D. R. Doelling, 1995: Cloud properties derived from GOES-7 for the spring 1994 ARM Intensive Observing Period using Version 1.0.0 of the ARM Satellite Data Analysis Program. *NASA RP 1366*, August, 59 pp.